Chemistry & Biology, Vol. 12, 1221–1226, November, 2005, ©2005 Elsevier Ltd All rights reserved. DOI 10.1016/j.chembiol.2005.09.006

Ligand Requirements for *glmS* Ribozyme Self-Cleavage

Tom J. McCarthy,[1] Melissa A. Plog,[1] Shennen A. Floy,[1] Joshua A. Jansen,[1] Juliane K. Soukup,[1,*] and Garrett A. Soukup[2,*]
[1]Department of Chemistry
Creighton University
[2]Department of Biomedical Sciences
Creighton University School of Medicine
2500 California Plaza
Omaha, Nebraska, 68178

Summary

Natural RNA catalysts (ribozymes) perform essential reactions in biological RNA processing and protein synthesis, whereby catalysis is intrinsic to RNA structure alone or in combination with metal ion cofactors. The recently discovered *glmS* ribozyme is unique in that it functions as a glucosamine-6-phosphate (GlcN6P)-dependent catalyst believed to enable "riboswitch" regulation of amino-sugar biosynthesis in certain prokaryotes. However, it is unclear whether GlcN6P functions as an effector or coenzyme to promote ribozyme self-cleavage. Herein, we demonstrate that ligand is absolutely requisite for *glmS* ribozyme self-cleavage activity. Furthermore, catalysis both requires and is dependent upon the acid dissociation constant (pK_a) of the amine functionality of GlcN6P and related compounds. The data demonstrate that ligand is integral to catalysis, consistent with a coenzyme role for GlcN6P and illustrating an expanded capacity for biological RNA catalysis.

Introduction

The majority of natural ribozymes perform RNA cleavage or splicing through transesterification reactions that utilize an internal or external hydroxyl group for nucleophilic attack on the phosphate at the cleavage or splice site [1–3]. Mechanistic strategies that ribozymes employ to promote RNA transesterification include metal-ion catalysis and/or general acid-base catalysis utilizing internal functional groups, as indicated by the self-cleaving hammerhead [4–6], HDV [7–9], hairpin [10–12], and VS [13, 14] ribozymes. Although self-splicing group I introns utilize exogenous guanosine as a nucleophilic substrate [2], catalysis is likewise attributable to intrinsic RNA structure and metal ion cofactors [15].

Recent discoveries of two ligand-responsive, self-cleaving ribozymes [16, 17] suggest that the scope of biological RNA catalysis might extend beyond the intrinsic capabilities of RNA by harnessing ligand functionalities. The cotranscriptional cleavage (CoTC) element in the 3′ untranslated region (UTR) of human β-globin mRNA contains a guanosine-sensitive ribozyme that promotes self-cleavage [17] and exonuclease-mediated transcriptional termination [18]. The products of β-globin ribozyme cleavage possess 5′-phosphate and 3′-hydroxyl termini that do not incorporate guanosine [17]. The *glmS* ribozyme [16] is categorized as a unique member of otherwise noncatalytic "riboswitches" that function as metabolite-dependent genetic regulatory elements [19]. The *glmS* ribozyme resides in the 5′ UTR of *glmS* mRNA in certain prokaryotes [20] and represses gene expression when activated by glucosamine-6-phosphate (GlcN6P) [16], the metabolic product of the GlmS enzyme. The products of *glmS* ribozyme cleavage possess 5′-hydroxyl and 2′,3′-cyclic phosphate termini that do not incorporate GlcN6P [16]. While both the β-globin and *glmS* ribozymes are activated by binding nonsubstrate organic compounds, it is presently unclear how such ligands function to activate catalysis.

Two fundamental strategies that greatly enhance the proficiency and functionality of protein enzymes in biological catalysis include exogenous organic compounds as requisite participants in catalysis (i.e., coenzymes) or as allosteric effectors that modulate enzymatic activity. Although effector- and coenzyme-dependent functions have been explored in the context of engineered allosteric ribozymes [21] and artificial nucleic acid catalysts [22, 23], such mechanistic distinctions have not yet been applied to naturally occurring, ligand-dependent ribozymes. To gain a better understanding of how GlcN6P might promote *glmS* ribozyme activity as either an effector or a coenzyme, we have examined the ligand requirements for *glmS* ribozyme self-cleavage.

Results and Discussion

To discriminate between the potential roles for GlcN6P in the mechanism of *glmS* ribozyme self-cleavage, we have examined the self-cleavage activity of the *glmS* ribozyme derived from *Bacillus cereus* (Figure 1A). The *glmS* ribozyme contains four paired domains (P1–P4) that are highly conserved among an 18-member phylogeny [20]. Previous characterization of the *B. subtilis glmS* ribozyme demonstrated that the minimal segment required to establish GlcN6P-dependent self-cleavage activity encompasses nucleotides from the +1 position (relative to the cleavage site) through the P2 domain, while the P3–P4 domains serve to enhance activity [16]. For the full-length *B. subtilis glmS* ribozyme, GlcN6P binding was reported to elicit a 1000-fold increase in the observed rate constant (k_{obs}) for self-cleavage activity under saturating GlcN6P and divalent metal ion concentrations [16]. However, our analysis of the *B. cereus glmS* ribozyme reveals that GlcN6P is more vital to self-cleavage activity than previously appreciated.

Reaction of the P1–P4 *B. cereus glmS* ribozyme in the absence or presence of GlcN6P (Figure 1B) demonstrates that the ribozyme possesses considerable self-cleavage activity in the absence of ligand in TRIS-buffered solution as previously reported [16]. To the contrary, the ribozyme is largely devoid of self-cleavage activity in HEPES-buffered solution in the absence of GlcN6P (Figure 1B), demonstrating a greater dependence

*Correspondence: jksoukup@creighton.edu (J.K.S.); gasoukup@creighton.edu (G.A.S.)

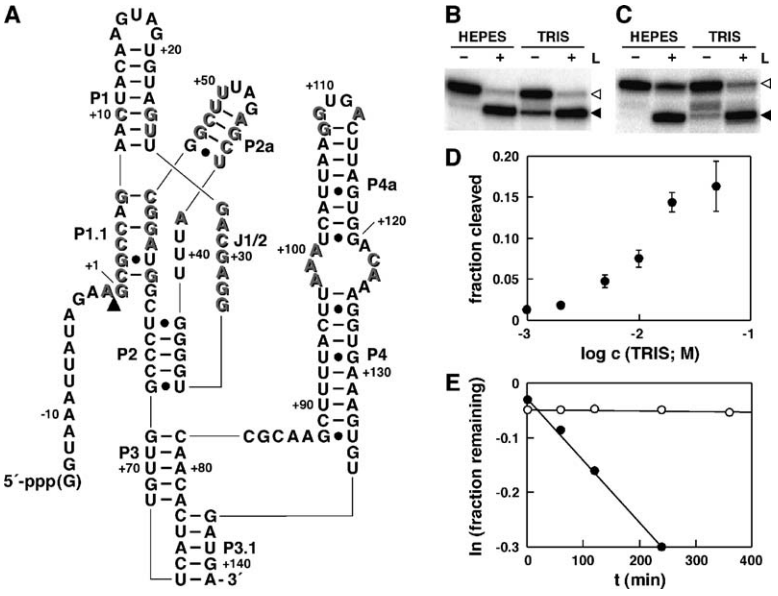

Figure 1. *glmS* Ribozyme Structure and TRIS-Activated Self-Cleavage

(A) Refined secondary structure model of the *B. cereus glmS* ribozyme containing nucleotides −13 through +141 relative to the cleavage site (arrowhead). An additional 5′-terminal guanosine at −14 (parentheses) was included to facilitate in vitro transcription. Depicted are paired regions P1–P4 including a putative 5′-proximal pseudoknot (P1.1) supported by mutational analysis (G.A.S., unpublished data) and a 3′-proximal pseudoknot (P3.1) indicated by phylogenetic analysis (R.R. Breaker, personal communication). Nucleotide identities that are ≥95% conserved are highlighted.

(B) TRIS-activated self-cleavage of the *glmS* ribozyme. Shown are products of reactions incubated for 2 hr in the absence (−) or presence (+) of 200 μM GlcN6P (L) under standard conditions (HEPES) or standard conditions substituting HEPES with TRIS (TRIS). Bands corresponding to the ribozyme (open arrowhead) and its 3′ cleavage product (filled arrowhead) are indicated.

(C) TRIS-activated self-cleavage of a truncated P1-P3 *glmS* ribozyme. A construct containing nucleotides −13 through +86 of the *B. cereus glmS* ribozyme was prepared and analyzed as in (B).

(D) Dependence of glmS ribozyme self-cleavage on TRIS concentration. Depicted is the fraction of ribozyme cleaved in reactions incubated for 2 h under standard conditions replacing HEPES with HEPES:TRIS in millimolar ratios from 49:1 to 0:50 as indicated by TRIS concentration alone. Error bars indicate the standard deviation determined for two replicate assays.

(E) Rate of *glmS* ribozyme self-cleavage in the absence (open circle) or presence (filled circle) of 10 mM TRIS as ligand under standard conditions.

upon GlcN6P. Similar analysis of a truncated P1–P3 ribozyme (Figure 1C) demonstrates that TRIS-activated self-cleavage is more pronounced for the P1–P4 ribozyme, consistent with the previous observation that the P3–P4 domains function to enhance activity [16]. By varying the molar ratio of HEPES:TRIS in otherwise equivalently buffered solutions (Figure 1D), it is evident that the self-cleavage activity of the P1–P4 ribozyme responds to TRIS concentration in a manner similar to GlcN6P-dependent activation [16]. These data indicate that TRIS can functionally substitute for GlcN6P, although it appears to be a lower-affinity ligand incapable of saturating the catalyst at concentrations ≤ 50 mM. Determination of k_{obs} values for ribozyme self-cleavage in the absence or presence of TRIS (Figure 1E) demonstrates that 10 mM TRIS accounts for a rate enhancement of 130-fold over the background k_{obs} of $\sim 10^{-5}$ min^{-1}. By comparison, saturating 10 mM GlcN6P elicits a k_{obs} of 1.1 min^{-1}, revealing that the true rate enhancement provided by GlcN6P binding to the *glmS* ribozyme is approximately five orders of magnitude (Table 1). Importantly, the background k_{obs} for the ribozyme is consistent with that for uncatalyzed transesterification of an unconstrained phosphodiester linkage or a constrained in-line linkage [24], suggesting that the catalytic mechanism of the *glmS* ribozyme is intrinsically linked to GlcN6P.

Table 1. Kinetic Parameters for the *glmS* Ribozyme in the Absence or Presence of 10 mM GlcN6P or Various Analogs under Standard Conditions

Ligand	k_{obs} (min^{-1})	Apparent K_D (mM)	Rate Enhancement
GlcN6P	1.1	0.03	110,000
GlcN	3.0×10^{-2}	≥5	3,000
Serinol	7.5×10^{-3}	≥5	750
TRIS	1.3×10^{-3}	≥25	130
—	$\sim 10^{-5}$	—	—

In consideration of a molecular basis for TRIS-dependent *glmS* ribozyme self-cleavage, it becomes apparent that TRIS structure is analogous to the amine-containing portion of GlcN6P, thereby implicating the importance of the amine functionality in ligand binding and activation of self-cleavage. An analysis of GlcN6P and related compounds (Figure 2A) reveals a striking dependence of ribozyme activity upon amine-containing analogs (Figure 2B). Both GlcN6P and glucosamine (GlcN) activate *glmS* ribozyme self-cleavage, while glucose-6-phosphate (Glc6P) and glucose (Glc) do not. In these reactions, GlcN is less than two orders of magnitude less potent than GlcN6P as an activator (Table 1). These data demonstrate that the phosphate moiety of GlcN6P is partially expendable with regard to binding and catalysis, while the amine functionality is vital. Further examination of amine-containing analogs reveals the simplicity of ligand recognition and catalysis (Figures 2A and 2B). Serinol, a more precise analog of GlcN6P than TRIS, expectedly functions as a more potent activator of ribozyme activity (Table 1), while trimethylene glycol (TMG), an analog lacking the amine group, fails to elicit ribozyme self-cleavage. Interestingly, L-serine (L-Ser) supports ribozyme activity, while D-serine (D-Ser) does not. These compounds demonstrate that stereochemical presentation of amine and hydroxyl functionalities might be an important determinant of ligand recognition and catalysis, and they implicate the importance of the C1 hydroxyl of GlcN6P. Moreover, adjacent amine and hydroxyl functionalities establish the minimal requirement for activity, as ethanolamine (EtOHN) supports ribozyme

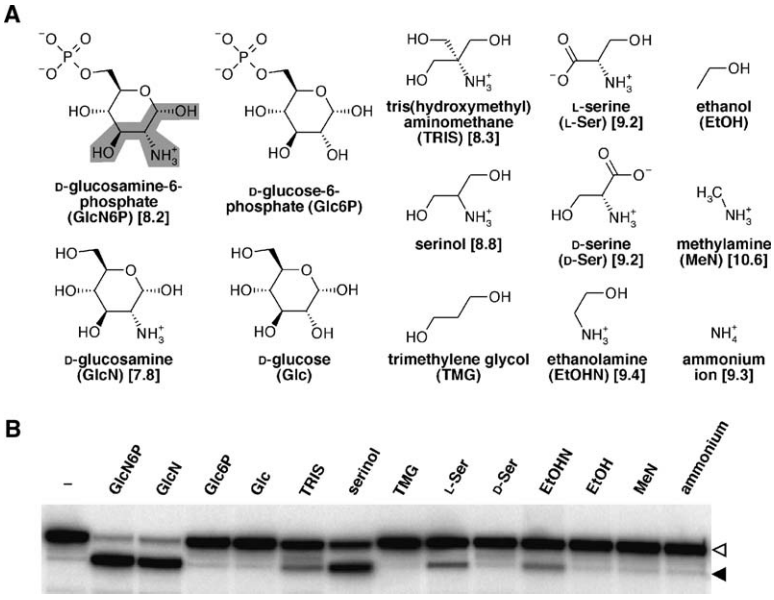

Figure 2. Dependence of *glmS* Ribozyme Self-Cleavage on Amine-Containing Analogs of GlcN6P

(A) Chemical structures of GlcN6P and related compounds depicted as the predominant species at pH 7.5. The portion of GlcN6P mimicked by other amine-containing compounds is shaded. Shown in brackets is the pK_a of each amine functionality taken from product literature or experimentally determined (Figure S1).

(B) Ligand-activated *glmS* ribozyme self-cleavage. Shown are products of reactions incubated for 2 hr under standard conditions in the absence (–) or presence of 200 μM GlcN6P or 10 mM analog as indicated. Bands corresponding to the ribozyme (open arrowhead) and its 3′ cleavage product (filled arrowhead) are indicated.

self-cleavage, while ethanol (EtOH), methylamine (MeN), and ammonium ion do not. These data clearly demonstrate the *glmS* ribozyme's minimal, but rigid, chemical requirement of ligand to perform catalysis.

Discriminating between the effects of functional group substitutions on ligand binding versus catalysis is a formidable challenge. This is particularly the case for GlcN6P activation of the *glmS* ribozyme, where there appear to be few determinants for ligand recognition and catalysis that likely attribute to the relatively poor apparent dissociation constant (K_D) determined for GlcN6P [16]. Hydroxyl group substitution of the amine functionality by Glc6P does not entirely preclude the possibility of hydrogen bonding at the affected position (i.e., binding). However, the relatively greater acid dissociation constant (pK_a) of the hydroxyl group markedly reduces the potential of Glc6P to accept or donate a proton in potential mechanisms of catalysis. Indeed, Glc6P is observed to function as an inhibitor of analog-dependent *glmS* ribozyme self-cleavage (Figure 3A). The extent of inhibition likely reflects the relative binding affinity of each analog versus that of Glc6P, as TRIS-, L-Ser-, and EtOHN-dependent self-cleavage are more easily inhibited with Glc6P than are GlcN- and serinol-dependent self-cleavage. While Glc6P is unable to affect saturating, GlcN6P-dependent self-cleavage (Figure 3A), it does effectively inhibit nonsaturating, GlcN6P-dependent self-cleavage with an apparent K_i of 3.0 mM (Figure 3B). Therefore, Glc6P exhibits competitive inhibition of GlcN6P, demonstrating competence in binding, but not catalysis. The absolute inability of the hydroxyl group substitution to support catalysis in Glc6P-ribozyme complexes suggests that the role of the amine functionality in GlcN6P-activated self-cleavage goes beyond an effect of binding. The data, therefore, demonstrate that the amine functionality is more important to catalysis than binding per se, and they suggest that GlcN6P might act as a coenzyme in *glmS* ribozyme self-cleavage.

The hypothesis that coenzyme function of GlcN6P in *glmS* ribozyme self-cleavage involves participation of

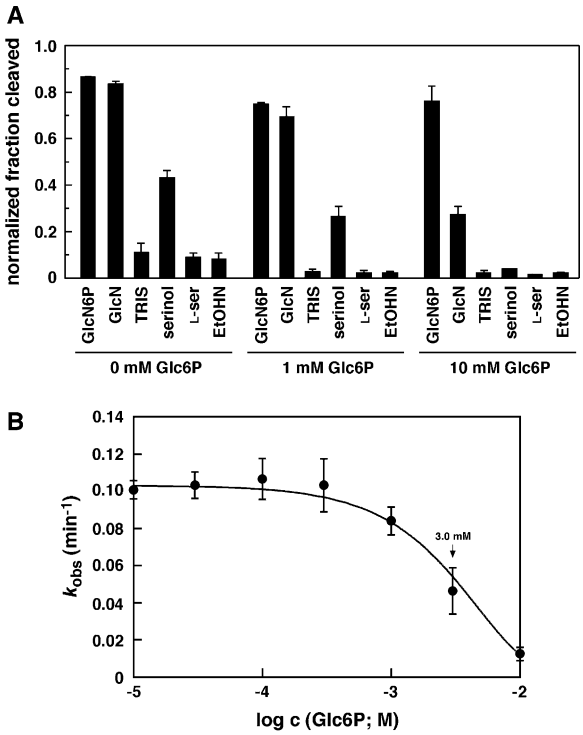

Figure 3. Competitive Inhibition of *glmS* Ribozyme Self-Cleavage by Glc6P

(A) Competition of ligand-activated ribozyme activity by Glc6P. Depicted is the fraction of ribozyme cleaved in reactions incubated for 2 hr under standard conditions including 10 mM ligand and 0, 1, or 10 mM Glc6P as indicated. Fraction cleaved was normalized to reaction lacking ligand, and error bars indicate the standard deviation determined for two replicate assays.

(B) Competition of GlcN6P-activated ribozyme activity by Glc6P. Reactions were performed under standard conditions with 10 μM GlcN6P and various concentrations of Glc6P. The concentration of Glc6P required to achieve a half-maximal k_{obs} value (apparent K_i) is indicated. Error bars indicate the standard deviation determined for three replicate assays.

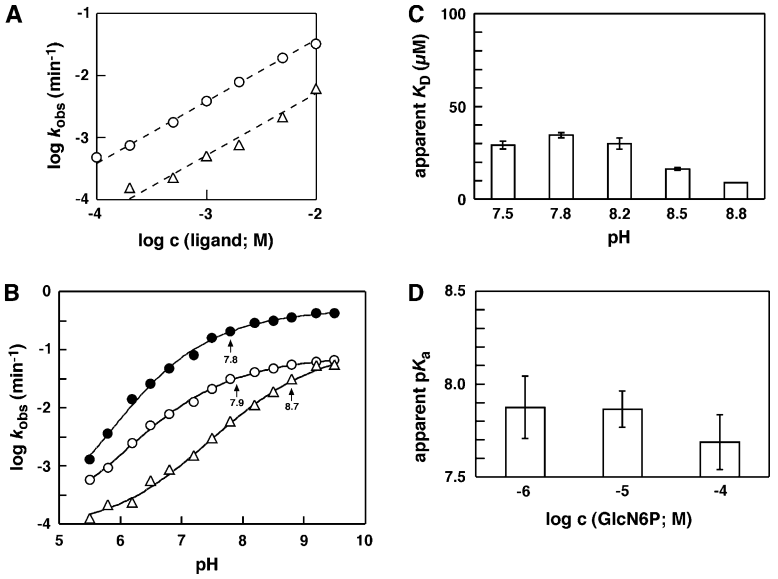

Figure 4. Reactivity Profiles of Ligand-Activated *glmS* Ribozyme Self-Cleavage

(A) Ligand concentration dependence. Reactions were performed under standard conditions with various concentrations of GlcN (open circles) or serinol (open triangles). Dashed lines represent a slope of 1. Data depicted are representative of two replicate assays.

(B) pH dependence. Reactions were performed under standard conditions using 10 mM GlcN (open circles) or serinol (open triangles), and substituting HEPES with other non-amine-containing buffering agents as appropriate to maintain the desired pH. Reactions were similarly performed using 10 μM GlcN6P (filled circles). The pH required to achieve a half-maximal k_{obs} value (apparent pK_a) is indicated for each ligand. Data depicted are representative of two replicate assays.

(C) pH dependence of apparent K_D for GlcN6P. The bar graph summarizes apparent K_D values determined for GlcN6P under standard conditions at various pH (Figure S2A).

(D) GlcN6P concentration dependence of apparent pK_a. The bar graph summarizes apparent pK_a values determined for various concentrations of GlcN6P under standard conditions (Figure S2B). Error bars indicate the standard deviation determined for two replicate assays.

the amine functionality in proton transfer predicts that ribozyme activity is necessarily dependent upon the pK_a of the amine group. Advantageously, pK_a values determined for GlcN and serinol (Figure S1A; see the Supplemental Data available with this article online) differ by ~1 (Figure 2A), thereby enabling a facile means of assessing coenzyme function by examining the reactivity profiles of ribozyme with each ligand. At constant pH, varying the concentration of GlcN or serinol produces a linear reactivity profile with a slope of ~1 (Figure 4A), demonstrating that ribozyme is not saturated at GlcN or serinol concentrations $\leq$ 10 mM, but consistent with previous data for GlcN6P demonstrating that activation results from a single binding event [16]. Moreover, the reactivity profiles for GlcN and serinol exhibit a relative shift by one log unit ligand concentration. This shift is likely attributable to the unit difference in pK_a between the two ligands (i.e., log unit difference in the concentration of deprotonated species at constant pH below pK_a), and it suggests that deprotonated ligand is the effective activator. Accordingly, the reactivity profiles generated by varying pH with constant GlcN or serinol concentration (Figure 4B) exhibit a slope of ~1 and a relative shift by one pH unit under reaction conditions where pH does not exceed the pK_a of either compound. These data demonstrate that there is a single deprotonation event for GlcN or serinol that influences ribozyme activity and corresponds with the established unit difference in pK_a between the two compounds. Importantly, reactivity reaches a near identical maximum under conditions where pH exceeds the pK_a of each compound, demonstrating that fully deprotonated GlcN and serinol function equivalently with regard to binding and activation of catalysis. Moreover, the approximate pH required for each ligand to elicit a half-maximal rate constant for self-cleavage (apparent pK_a; Figure 4B) corresponds closely to the pK_a values of each compound. Reactivity profiles therefore demonstrate a relationship between the protonation state of ligand and ribozyme activity that support a role for ligand as a coenzyme in potential mechanisms involving proton transfer.

Interestingly, the reactivity profile for *glmS* ribozyme activation by GlcN6P exhibits a markedly different relationship with pH (Figure 4B). The pH-reactivity profile was examined with nonsaturating GlcN6P, where the apparent pK_a is 7.8. Importantly, the amine functionality of GlcN6P alone exhibits a pK_a of 8.2 (Figure S1B). The data, therefore, suggest that the pK_a of GlcN6P is perturbed slightly toward neutrality in the context of the ribozyme; a feature expected to enhance catalysis. Considering that the ribozyme appears incapable of similarly affecting the pK_a of either GlcN or serinol as ligand analogs suggests that it works specifically in concert with GlcN6P to maximize catalysis. While the phosphate moiety of GlcN6P enhances binding affinity (Table 1), interaction of the ligand with the ribozyme might "mask" the proximity effect of the phosphate group on the pK_a of the amine functionality, thereby yielding an apparent pK_a for GlcN6P that is consistent with the apparent and actual pK_a values for GlcN (Figure 4B and Figure S1A). Importantly, the apparent pK_a for the GlcN6P-stimulated reaction likely accurately reflects the pK_a of GlcN6P rather than an effect of the protonation state upon ligand binding affinity, as the apparent K_D for GlcN6P is affected only 3-fold by pH over a range that corresponds to a 20-fold difference in the ratio of deprotonated and protonated GlcN6P in solution (Figure 4C and Figure S2A). Moreover, the apparent pK_a of the reaction is not affected by GlcN6P concentration (Figure 4D and Figure S2B). The data demonstrate that the

protonation state of the amine functionality has a marginal effect on ligand binding although it is crucial to catalysis, and therefore support the possibility that ligand affects catalysis through its capacity for proton transfer rather than binding alone. Consequently, the data are consistent with the hypothesis that GlcN6P functions as a coenzyme rather than an effector in *glmS* ribozyme self-cleavage.

Significance

Our analysis of the GlcN6P-dependent *glmS* ribozyme demonstrates that self-cleavage is completely dependent upon the addition of amine-containing ligands, suggesting that the RNA alone lacks an intact catalytic site. Activation by GlcN6P achieves a rate enhancement of 110,000-fold, a value far greater than that which would be necessary to achieve a biological effect upon a typical bacterial mRNA with a half-life of only minutes. Moreover, reactivity profiles demonstrate that ligand-activated catalysis is dependent upon the pK_a of the amine functionality, while ligand binding affinity appears to be only modestly affected by the protonation state. The data are therefore consistent with the hypothesis that GlcN6P functions as a coenzyme for *glmS* ribozyme self-cleavage rather than an allosteric effector that modulates catalytic activity. A probable mechanistic role for ligand includes amine-mediated proton transfer that promotes general acid-base catalysis similar to the role of cytosine in HDV ribozyme self-cleavage [7–9]. However, additional studies will be required to elucidate the precise interactions between ligand and the *glmS* ribozyme that contribute to catalysis.

The *glmS* ribozyme serves as an illustration that a natural RNA catalyst can exploit organic compounds to achieve catalytic competency and enhance biological functionality, underscoring the possibility that additional such catalysts are likely to exist in nature although their identification is made challenging by the necessity to reconstitute appropriate holoenzymatic complexes. The ability of nucleic acid catalysts to utilize coenzymes has only been demonstrated previously by artificial activities [22, 23], and it supports the notion that modern biology might have evolved from a sophisticated "RNA world." The *glmS* ribozyme, however, demonstrates that contemporary RNA catalysts can be equally sophisticated in their function, placing ribozymes more on par with their protein enzyme counterparts.

Experimental Procedures

Templates for transcription were prepared by primer extension and PCR amplification by using synthetic DNA corresponding to ribozyme sequence. Ribozymes were prepared by in vitro transcription with T7 RNA polymerase and ^{32}P-labeling by incorporation of [α-^{32}P]-UTP. Transcription products were separated by denaturing 10% polyacrylamide gel electrophoresis (PAGE), and ribozymes were eluted in solution containing 50 mM HEPES (pH 7.5 at 23ºC) and 200 mM NaCl, precipitated with ethanol, and redissolved in water.

Ribozyme reactions contained $\leq$250 nM ribozyme and ligand as indicated, and they were performed under standard conditions consisting of incubation at 23ºC in solution containing 50 mM HEPES (pH 7.5 at 23ºC) and 10 mM $MgCl_2$, except as noted otherwise. TRIS, MES, PIPES, TAPS, or CHES was substituted for HEPES as indicated. Reactions were terminated by the addition of a gel loading dye containing 10 M urea and 20 mM EDTA. Products were separated by denaturing 10% PAGE and were analyzed with a PhosphorImager and IMAGEQUANT software (Molecular Dynamics). k_{obs} values for self-cleavage were derived by plotting the natural logarithm of the fraction of uncleaved ribozyme versus time and establishing the negative slope of the resulting line. Stated values represent the average of two replicate assays. Apparent K_i was established by fitting data from three replicate assays to an exponential curve. Apparent K_D values were established by fitting average data from at least two replicate assays to the Michaelis-Menten equation: $k_{obs} = (k_{max} \times [ligand])/([ligand] + \text{apparent } K_D)$. Apparent pK_a values were determined by fitting average data from at least two replicate assays to the Hill equation: $k_{obs} = (k_{max} \times pH^n)/(pH^n + \text{apparent } pK_a^n)$, where *n* represents the Hill coefficient.

Supplemental Data

Supplemental Data including potentiometric titration curves for pK_a determination and kinetic analyses for apparent pK_a and apparent K_D determination are available at http://www.chembiol.com/cgi/content/full/12/11/1221/DC1/.

Acknowledgments

We especially thank R.R. Breaker for critical comments and suggestions, and we thank A. Roth and M. Hulce for helpful discussions. J.K.S. is supported by the Clare Boothe Luce Program of the Henry Luce Foundation and National Institutes of Heath (NIH) grant P20 RR16469 from the Institutional Development Award Program for Networks of Biomedical Research Excellence Program of the National Center for Research Resources (NCRR). G.A.S. is supported by the Health Future Foundation and NIH grant P20 RR017717 from the Centers of Biomedical Research Excellence Program of the NCRR. This investigation was in part conducted in a facility constructed with support from NIH grant C06 RR17417 from the Research Facilities Improvement Program of the NCRR.

Received: August 16, 2005
Revised: September 8, 2005
Accepted: September 9, 2005
Published: November 18, 2005

References

1. Frank, D.N., and Pace, N.R. (1998). Ribonuclease P: unity and diversity in a tRNA processing ribozyme. Annu. Rev. Biochem. *67*, 153–180.
2. Doudna, J.A., and Cech, T.R. (2002). The chemical repertoire of natural ribozymes. Nature *418*, 222–228.
3. Moore, P.B., and Steitz, T.A. (2003). The structural basis of large ribosomal subunit function. Annu. Rev. Biochem. *72*, 813–850.
4. Murray, J.B., Seyhan, A.A., Walter, N.G., Burke, J.M., and Scott, W.G. (1998). The hammerhead, hairpin and VS ribozymes are catalytically proficient in monovalent cations alone. Chem. Biol. *5*, 587–595.
5. O'Rear, J.L., Wang, S., Feig, A.L., Beigelman, L., Uhlenbeck, O.C., and Herschlag, D. (2001). Comparison of the hammerhead cleavage reactions stimulated by monovalent and divalent cations. RNA *7*, 537–545.
6. Curtis, E.A., and Bartel, D.P. (2001). The hammerhead cleavage reaction in monovalent cations. RNA *7*, 546–552.
7. Ferre-D'Amare, A.R., and Doudna, J.A. (1998). Crystal structure of a hepatitis delta virus ribozyme. Nature *395*, 567–574.
8. Nakano, S., Chadalavada, D.M., and Bevilacqua, P.C. (2000). General acid-base catalysis in the mechanism of a hepatitis delta virus ribozyme. Science *287*, 1492–1497.
9. Shih, I.H., and Been, M.D. (2001). Involvement of a cytosine side chain in proton transfer in the rate-determining step of ribozyme self-cleavage. Proc. Natl. Acad. Sci. USA *98*, 1489–1494.
10. Rupert, P.B., and Ferre-D'Amare, A.R. (2001). Crystal structure of a hairpin ribozyme-inhibitor complex with implications for catalysis. Nature *410*, 780–786.

11. Rupert, P.B., Massey, A.P., Sigurdsson, S.T., and Ferre-D'Amare, A.R. (2002). Transition state stabilization by a catalytic RNA. Science *298*, 1421–1424.
12. Bevilacqua, P.C. (2003). Mechanistic considerations for general acid-base catalysis by RNA: revisiting the mechanism of the hairpin ribozyme. Biochemistry *42*, 2259–2265.
13. Jones, F.D., and Strobel, S.A. (2003). Ionization of a critical adenosine residue in the neurospora Varkud Satellite ribozyme active site. Biochemistry *42*, 4265–4276.
14. Lilley, D.M. (2004). The Varkud satellite ribozyme. RNA *10*, 151–158.
15. Adams, P.L., Stahley, M.R., Kosek, A.B., Wang, J., and Strobel, S.A. (2004). Crystal structure of a self-splicing group I intron with both exons. Nature *430*, 45–50.
16. Winkler, W.C., Nahvi, A., Roth, A., Collins, J.A., and Breaker, R.R. (2004). Control of gene expression by a natural metabolite-responsive ribozyme. Nature *428*, 281–286.
17. Teixeira, A., Tahiri-Alaoui, A., West, S., Thomas, B., Ramadass, A., Martianov, I., Dye, M., James, W., Proudfoot, N.J., and Akoulitchev, A. (2004). Autocatalytic RNA cleavage in the human β-globin pre-mRNA promotes transcription termination. Nature *432*, 526–530.
18. West, S., Gromak, N., and Proudfoot, N.J. (2004). Human 5′ → 3′ exonuclease Xrn2 promotes transcription termination at co-transcriptional cleavage sites. Nature *432*, 522–525.
19. Mandal, M., and Breaker, R.R. (2004). Gene regulation by riboswitches. Nat. Rev. Mol. Cell Biol. *5*, 451–463.
20. Barrick, J.E., Corbino, K.A., Winkler, W.C., Nahvi, A., Mandal, M., Collins, J., Lee, M., Roth, A., Sudarsan, N., Jona, I., et al. (2004). New RNA motifs suggest an expanded scope for riboswitches in bacterial genetic control. Proc. Natl. Acad. Sci. USA *101*, 6421–6426.
21. Silverman, S.K. (2003). Rube Goldberg goes (ribo)nuclear? Molecular switches and sensors made from RNA. RNA *9*, 377–383.
22. Jadhav, V.R., and Yarus, M. (2002). Coenzymes as coribozymes. Biochemie *84*, 877–888.
23. Roth, A., and Breaker, R.R. (1998). An amino acid as a cofactor for a catalytic polynucleotide. Proc. Natl. Acad. Sci. USA *95*, 6027–6031.
24. Soukup, G.A., and Breaker, R.R. (1999). Relationship between internucleotide linkage geometry and the stability of RNA. RNA *5*, 1308–1325.